Wideband perfect absorption in arrays of tilted carbon nanotubes

S. M. Hashemi[1,2] and I. S. Nefedov[1]

[1]*Aalto University, School of Electrical Engineering, SMARAD Center of Excellence, P.O. Box 13000, 00076 Aalto, Finland*

[2]*Iran University of Science and Technology, Department of Electrical Engineering, Tehran 1684613114, Iran*

(Received 26 June 2012; revised manuscript received 18 October 2012; published 6 November 2012)

In this paper we discuss an interesting property of arrays of metallic carbon nanotubes, namely, the capability of perfect absorption in optically ultrathin layers. The carbon nanotube array is used in a regime where it possesses properties of a uniaxial indefinite medium. We show that if the optical axis is tilted with respect to an interface, a plane incident wave propagates inside a finite-thickness slab of the carbon nanotube array with a very small wavelength and small material losses cause the total wave absorption. We demonstrate that perfect matching with free space can be achieved in an optically ultrathin layer without a magnetic response and when the reflected wave is absent. Nonsymmetry appearing as a difference between wave numbers of waves propagating upward and downward with respect to the interface under oblique incidence leads to the absence of a thickness resonance.

DOI: 10.1103/PhysRevB.86.195411 PACS number(s): 78.67.Pt, 61.48.De, 42.25.Bs, 78.20.Ci

I. INTRODUCTION

Recently perfect absorption was demonstrated at far-infrared,[1] mid-infrared,[2] near-infrared,[3] and visible[4] frequencies. This paper is focused on the terahertz range. Many materials possess good absorption properties in the terahertz range. Nevertheless, the creation of optically ultrathin nonreflective absorbers is still a challenge. A high level of absorption can be achieved using resonant metamaterials.[5,6] Different metamaterials are utilized in each region and one of the most important tasks in the design of a perfect absorber is the impedance matching with free space. It can be achieved by exploiting the magnetic resonant response provided by the antiparallel surface currents in metal structures. Another approach, based on interference, was proposed in Ref. 7.

In this paper we describe the concept of the terahertz absorber, composed of a periodic array of parallel metallic carbon nanotubes. Carbon nanotube (CNT) films have found applications as absorbers for ultrafast broadband optical devices,[8] mode-locked lasers,[9] infrared thermal detectors,[10] etc. In these works no special properties of carbon nanotubes, excepting saturable absorption, are used. Almost full absorption in aligned single-wall carbon nanotubes was demonstrated across a very wide spectral range (0.2–200 μm) in Ref. 11, but the height of the CNT layer was 460 μm, which cannot be considered an optically thin layer. (Below we demonstrate that our approach allows achievement of full absorption within a considerably narrower spectral range, but at the slab thickness $\lambda/10$ only, where λ is the wavelength in free space.) Recently we have shown[12,13] that in the terahertz range arrays of parallel metallic carbon nanotubes exhibit properties of the *indefinite metamaterials* (IMs)[14]—uniaxial materials in which the axial and tangential components of the permittivity tensor have different signs. Our approach exploits a thin slab of the CNT indefinite medium, whose optical axis is tilted with respect to interfaces (see Fig. 1). We assume for simplicity that the CNT slab is grounded by the perfect electric conductor plane at $z = 0$.

The main properties of both single CNTs and CNT arrays are determined by their complex conductivity, where its imaginary part is comparable with the real part or even exceeds it.[15] It was shown in Refs. 13 and 16 that CNT arrays behave as ϵ-negative uniaxial crystals, whose axial component of the effective permittivity tensor is expressed by the Drude formula. Under certain conditions, described below, there is possible propagation of the Transverse Magnetic (TM) waves with extremely slow phase velocities and, consequently, very small wavelengths. Then such waves will attenuate in an ultrathin layer of even a low-loss medium. We show that the CNT array can be matched with free space if we arrange the carbon nanotubes under an angle of 45° with respect to the interface and reflection can be totally eliminated. Then perfect absorption can be achieved within an optically ultrathin layer.

This paper is organized as follows. In Sec. II we discuss properties of eigenwaves propagating in arrays of CNTs. Propagation constants and wave impedances of these waves with a fixed transverse component of the wave vector are needed for solution of the problem of a plane-wave reflection from a finite-thickness slab. If CNTs are tilted, wave-vector components are different for waves propagating upward and downward with respect to the interface. Of special interest is when one of them tends to infinity and the other tends to the normal component of the wave vector in free space. Conditions of perfect absorption are derived. Section III presents a solution of the wave-reflection problem using the transfer matrix method, modified for nonsymmetrical transmission lines, and discussion of numerical results.

II. EIGENWAVES IN CARBON NANOTUBE ARRAYS

Let us assume that single-wall carbon nanotubes are infinitely long in the z' direction and the CNT array is periodic in the x' and y' directions. As a model of the individual metallic zigzag nanotube we use an impedance cylinder, characterized by complex dynamic conductivity, and effective boundary conditions.[15] The carbon nanotube radius r is expressed via the dual index (m,n) and is given by

$$r = \frac{\sqrt{3}}{2\pi} b \sqrt{m^2 + mn + n^2}, \tag{1}$$

where $b = 0.142$ nm is the interatomic distance in graphene. For the metallic zigzag CNTs $n = 0$ and $m = 3q$, where q is an integer. So, the radius of the metallic zigzag CNT r reads as

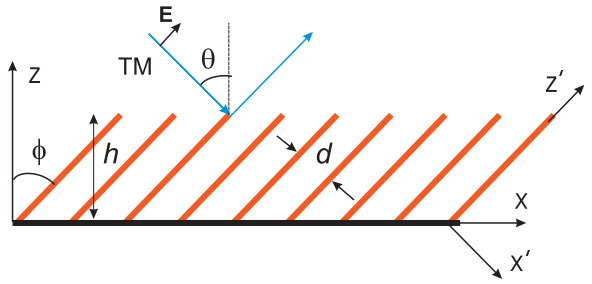

FIG. 1. (Color online) Schematic view of an indefinite-medium slab with the tilted optical axis.

$r = 3\sqrt{3}qb/2\pi$. The simple approximate expression for the axial component of the complex surface conductivity, which is valid for metallic zigzag CNTs in the frequency range below optical transitions, looks like

$$\sigma \cong -j\frac{2\sqrt{3}e^2\Gamma_0}{3q\pi\hbar^2(\omega - j\nu)}, \tag{2}$$

where e is the electron charge, $\Gamma_0 = 2.7$ eV is the overlapping integral, $\tau = 1/\nu$ is the relaxation time, and $\hbar$ is the reduced Planck constant. Since the wall of a single-wall CNT is a monatomic sheet of carbon, Eq. (2) can be considered the surface conductivity of the carbon nanotube. Simple formulas for the surface conductivity like Eq. (2) were used in many publications devoted to Electromagnetic (EM) properties of CNTs.[17–22] The surface impedance per unit length can be found as

$$z_i = \frac{1}{2\pi r\sigma} = \frac{\sqrt{3}q\hbar^2\nu}{4e^2\Gamma_0 r} + j\omega\frac{\sqrt{3}q\hbar^2}{4e^2\Gamma_0 r} = R_0 + j\omega L_0, \tag{3}$$

where L_0 is the kinetic inductance. Actually, taking into account the expression for the Fermi velocity of the π electrons[21]

$$v_F = \frac{3\Gamma_0 b}{2\hbar} \tag{4}$$

and formula (1) for r, we come to the definition of the kinetic inductance, $L_{\rm kin} = \hbar\pi/(Me^2v_F)$,[23] where M is the number of quantum channels. There are four quantum channels in thin CNTs ($M = 4$): two spin-up and two spin-down channels (see Ref. 17).

Let us consider a two-dimensional periodic array of CNTs. In the coordinate system x', y', z' the relative permittivity dyadic reads as

$$\overline{\overline{\varepsilon}}' = \varepsilon'_{zz}\mathbf{z}'_0\mathbf{z}'_0 + \varepsilon_t(\mathbf{x}'_0\mathbf{x}'_0 + \mathbf{y}'_0\mathbf{y}'_0), \tag{5}$$

where ε_t is the transversal component of the permittivity dyadic. In the considered case of a low-density CNT array it is the permittivity of the host medium. Then for the CNT array we apply the effective medium model, developed for loaded wire media:[24]

$$\frac{\varepsilon'_{zz}}{\varepsilon_t} = 1 - \frac{k_p^2}{k^2 - j\xi k - k_{z'}^2/n^2}, \quad k_p^2 = \frac{\mu_0}{d^2 L_{\rm CNT}}, \tag{6}$$

where d is the period of the CNT array lattice, $k = k_0\sqrt{\varepsilon_t}$, k_0 is the wave number in free space; k_p is the effective plasma wave number; parameter $n^2 = L_{\rm CNT}C_{\rm CNT}/(\varepsilon_0\mu_0)$ measures the strength of spatial dispersion in the medium; $L_{\rm CNT}$ and $C_{\rm CNT}$ are the effective inductance and capacitance of CNTs per unit length, respectively; μ_0 and ε_0 are the permeability and permittivity of vacuum, respectively; and the parameter ξ is responsible for losses. The effective inductance contains the kinetic and the electromagnetic contributions and the last one can be neglected,[17] so we can take $L_{\rm CNT} = L_0$. The parameter of losses reads[13]

$$\xi = (R_0/L_{\rm CNT})\sqrt{\varepsilon_0\mu_0}. \tag{7}$$

The CNT capacitance is the quantum capacitance and it takes the form $C_{\rm CNT} = e^2/(\pi\hbar v_F)$. In the following calculations the relaxation time is taken to be $\tau = 10^{-13}$ s, the integer $q = 13$ [the dual index, characterizing the CNT, is (39,0)], so the radius of CNTs is $r \simeq 1.53$ nm. Let us estimate terms entering the denominator of Eq. (6) (see Refs. 13 and 16). Using the formulas given above, we obtain $n^2 \simeq 3.2 \times 10^4$. The value $k_{z'}/k$ can be quite large for eigenwaves;[12] however, it happens for very dense arrays ($d \sim 2$ nm) and under a very large transversal component of the wave vector $k_{x'}$ (close to edges of the Brillouin zones of the CNT lattice). In our case $k_{x'}$ is determined by $k_x = k\sin\theta$ and cannot be so large, so we can assume that this value is close to k. Thus, the spatial dispersion term $k_{z'}^2/n^2$ can be neglected for carbon nanotube arrays.

The permittivity dyadic of the CNT medium with CNTs, tilted in the XOZ plane, can be expressed through rotation transformation as

$$\overline{\overline{\varepsilon}} = \overline{\overline{U}}\,\overline{\overline{\varepsilon}}'\,\overline{\overline{U}}^T, \tag{8}$$

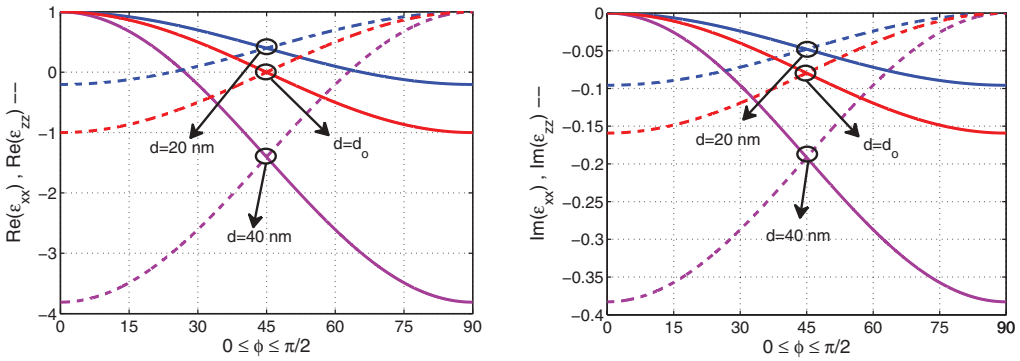

FIG. 2. (Color online) Real and imaginary parts of diagonal components of the relative permittivity dyadic for the CNT medium versus the tilt angle, calculated at the frequency $f = 20$ THz. $\mathrm{Re}(\varepsilon_{xx})$ and $\mathrm{Im}(\varepsilon_{xx})$ are shown by solid curves, $\mathrm{Re}(\varepsilon_{zz})$ and $\mathrm{Im}(\varepsilon_{zz})$ by dashed curves.

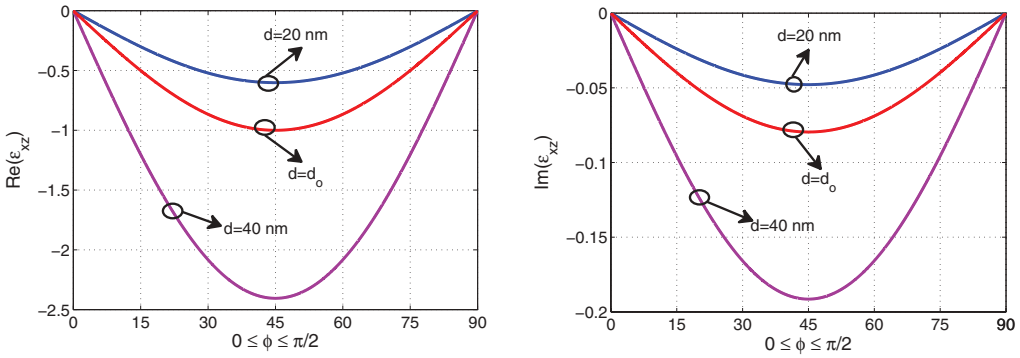

FIG. 3. (Color online) Real and imaginary parts of nondiagonal components of the relative permittivity dyadic for the CNT medium versus the tilt angle, calculated at $f = 20$ THz.

where the $\overline{\overline{\varepsilon}}'$ dyadic is the diagonal dyadic defined in Eq. (5), $\overline{\overline{U}}$ is the matrix of rotation around the y axis

$$\overline{\overline{U}} = \begin{bmatrix} \cos\phi & 0 & \sin\phi \\ 0 & 1 & 0 \\ -\sin\phi & 0 & \cos\phi \end{bmatrix}, \tag{9}$$

and $\overline{\overline{U}}^T$ is the transposed matrix. The Cartesian components of $\overline{\overline{\varepsilon}}'$ read

$$\begin{aligned} \varepsilon_{xz} &= \varepsilon_{zx} = (\varepsilon'_{zz} - \varepsilon_t)\cos\phi\sin\phi, \\ \varepsilon_{xx} &= \varepsilon'_{zz}\sin^2\phi + \varepsilon_t\cos^2\phi, \\ \varepsilon_{zz} &= \varepsilon'_{zz}\cos^2\phi + \varepsilon_t\sin^2\phi. \end{aligned} \tag{10}$$

One can find such $d = d_0$ that the permittivity dyadic components satisfy the condition of the indefinite medium, $\mathrm{Re}(\varepsilon'_{zz}) = -\mathrm{Re}(\varepsilon_t) = \varepsilon_{\mathrm{ind}}$. Since $\varepsilon_t = 1$ for the CNT array, $\varepsilon_{\mathrm{ind}} = -1$ in our case. We note that for $\phi = 45^\circ$ we obtain $\mathrm{Re}(\varepsilon_{zz}) = \mathrm{Re}(\varepsilon_{xx}) = 0$. The corresponding value of d can be computed as $d_0 = \sqrt{\mu_0/(2L_{\mathrm{CNT}}(k_0^2 + \xi^2))}$. For the taken parameter of losses at the frequency $f_0 = 20$ THz, imaginary parts of the permittivity dyadic components are the following: $\mathrm{Im}(\varepsilon'_{zz}) = -0.16$, $\mathrm{Im}(\varepsilon_{xz}) = \mathrm{Im}(\varepsilon_{xx}) = \mathrm{Im}(\varepsilon_{zz}) = -0.08$. Real and imaginary parts of diagonal and nondiagonal components of the permittivity dyadic, calculated for three different CNT lattice periods, are shown in Figs. 2 and 3. One can see that the absolute value of the relative permittivity decreases with increase of the lattice period.

To obtain eigenmodes propagating in the structure, we solve source-free Maxwell equations for TM waves using the constitutive relations for the tilted CNTs medium, and after eliminating the magnetic field, the equation for the electric field (eigenvalue equation) is obtained in the form

$$\begin{bmatrix} k_z^2 - k_0\varepsilon_{xx} & k_xk_z - k_0^2\varepsilon_{xz} \\ -k_xk_z + k_0\varepsilon_{xz} & -k_x^2 + k_0^2\varepsilon_{zz} \end{bmatrix} \begin{bmatrix} E_x \\ E_z \end{bmatrix} = 0. \tag{11}$$

The eigenvalues of Eq. (11) are the propagation constants of plane waves, propagating in the z direction under fixed k_x. They are evaluated as

$$k_z^{(1,2)} = \frac{k_x\varepsilon_{xz} \pm \sqrt{(\varepsilon_{xz}^2 - \varepsilon_{xx}\varepsilon_{zz})(k_x^2 - k_0^2\varepsilon_{zz})}}{\varepsilon_{zz}}. \tag{12}$$

In the particular case $d = d_0$,

$$k_z^{(1,2)} = \frac{-k_x\sqrt{1 - \varepsilon_{\mathrm{ind}}^2} \pm \sqrt{k_x^2 - k_0^2\varepsilon_{\mathrm{ind}}}}{\varepsilon_{\mathrm{ind}}}. \tag{13}$$

It can be seen from Eqs. (12) and (13) that there are two different values for k_z except in the case of the normal incidence $k_x = 0$. The incidence-angle dependence of real and imaginary parts of the normalized $k_z^{(1,2)}$ for $\phi = 45^\circ$, calculated

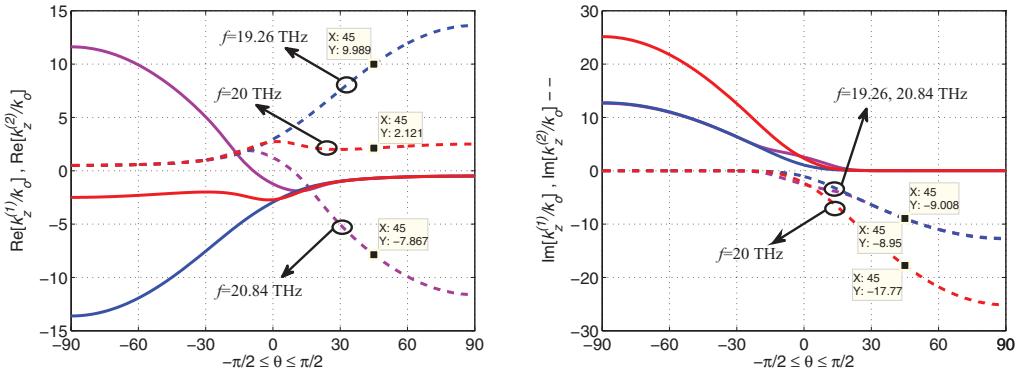

FIG. 4. (Color online) Real and imaginary parts of the normalized $k_z^{(1,2)}$ versus the incidence angle θ. Real and imaginary parts of $k_z^{(1)}$ and $k_z^{(2)}$ are shown by solid and dashed curves, respectively. The tilt angle is $\phi = 45^\circ$, and the period of the CNT array lattice is $d = d_0 = 31.12$ nm.

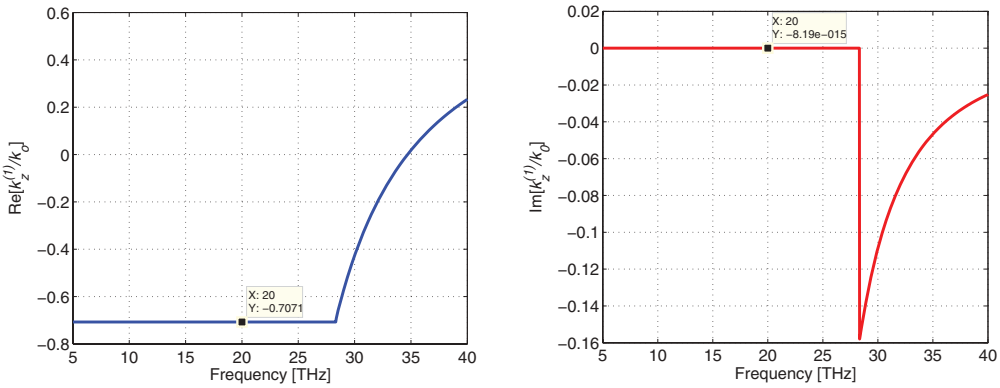

FIG. 5. (Color online) Frequency dependence of real and imaginary parts of the normalized $k_z^{(1)}$.

at different frequencies in the vicinity of f_0, are shown in Fig. 4. We can see that in one direction we have a large real part of $k_z^{(1)}$ and a lower value for $k_z^{(2)}$ and vice versa in the opposite direction. This effect of nonsymmetry takes place because at the fixed k_x the electric field vector of one wave has a larger projection to CNTs than that of another wave causing a different interaction between the field and the CNTs.

Let us consider the special case $\phi = 45^\circ$ and $\theta \to 45^\circ$. Then $\mathrm{Re}(\varepsilon_{xx}) = \mathrm{Re}(\varepsilon_{zz}) = \varepsilon_{\mathrm{ind}} = \delta \to 0$. To find the limiting transition for $k_z^{(1)}$, corresponding to the sign "+", we expand the second term of the numerator of Eq. (13) into the Taylor series under $\delta \to 0$, restricting expansion by the first small term, and obtain

$$k_z^{(1)} \simeq \frac{-k_x + k_0\left(\frac{k_x}{k_0} - \frac{k_0\delta}{2k_x}\right)}{\delta}, \tag{14}$$

so $k_z^{(1)} \to -k_0/\sqrt{2} = -k_0 \sin 45^\circ$ if $\delta \to 0$. With regard to the problem of the wave reflection from the slab (see Fig. 1), this eigenvalue corresponds to the wave reflected from the ground plane and propagating to the interface. It is equivalent to the z component of the wave vector in free space because its electric field vector is orthogonal to CNTs, which do not affect the wave propagation in this case. For the second wave number we come to $k_z^{(2)} \to -\infty$. This is explained by the facts that the electric field vector of the incident wave is parallel to CNTs and $\mathrm{Re}(\varepsilon'_{zz}) \to -1$ if $d \to d_0$. This wave propagates almost perpendicularly to the interface. It has the negative sign because it is the backward wave with respect to the interface (the wave deviates from the normal to the left side, i.e., in the carbon nanotubes direction). Figures 5 and 6 illustrate the frequency dependence of $k_z^{(1,2)}$ and show that both real and imaginary parts of $k_z^{(1)}$ remain constant at frequencies below $f_p \simeq 28$ THz with $|\mathrm{Re}(k_z^{(1)})| = k_0/\sqrt{2}$, where f_p is the plasmonic resonance frequency of the CNT array. For $k_z^{(2)}$ either the real or the imaginary part becomes quite large in the vicinity of f_0 for the lossy case.

The second remarkable feature concerns the transverse wave impedance $Z_{1,2}$, which reads as

$$Z_{1,2} = \frac{-E_x}{H_y} = \frac{\eta}{k_0}\frac{\sqrt{k_x^2 - k_0^2\varepsilon_{zz}}}{\sqrt{\varepsilon_{xz}^2 - \varepsilon_{xx}\varepsilon_{zz}}}, \tag{15}$$

where $\eta = 120\pi\ \Omega$. One can show that if $\phi = 45^\circ$ and $\theta = 45^\circ$ then

$$\varepsilon_{xz} = \varepsilon_{zx} = \tfrac{1}{2}(\varepsilon'_{zz} - \varepsilon_t), \quad \varepsilon_{xx} = \varepsilon_{zz} = \tfrac{1}{2}(\varepsilon'_{zz} + \varepsilon_t). \tag{16}$$

So, if $\varepsilon_t = 1$ we come to condition of perfect matching of transverse impedances of the plane wave, incident from free space,

$$Z_0 = \eta\frac{\sqrt{k_0^2 - k_x^2}}{k_0} = \eta\frac{1}{\sqrt{2}}, \tag{17}$$

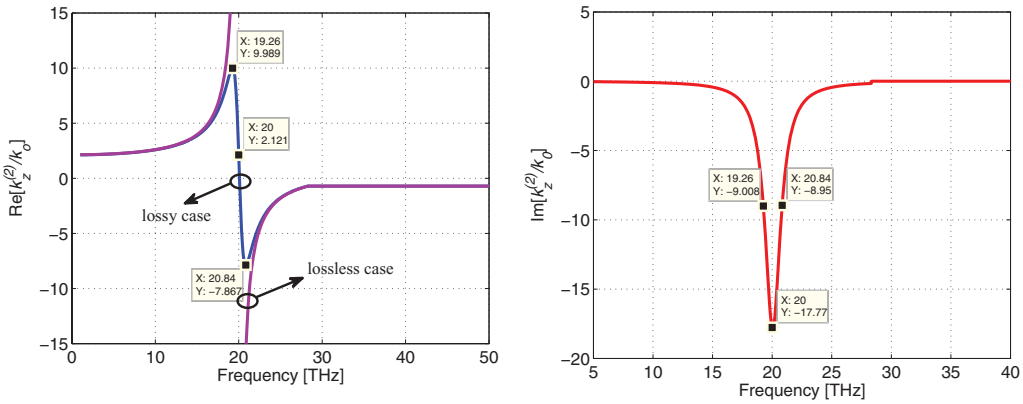

FIG. 6. (Color online) Frequency dependence of real and imaginary parts of the normalized $k_z^{(2)}$. $\mathrm{Re}(k_z^{(2)})$ for the lossless case also is shown.

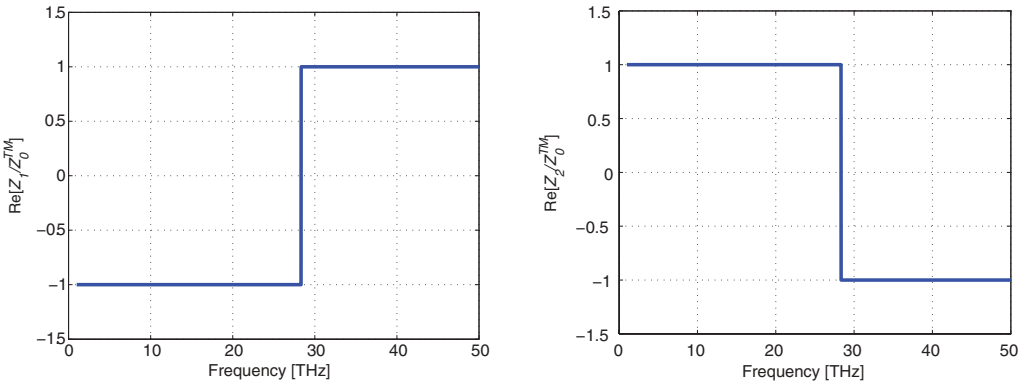

FIG. 7. (Color online) Real part of the normalized wave impedance versus frequency, calculated at $\phi = 45^\circ$, $\theta = 45^\circ$, and $d = d_0 = 31.12$ nm.

and both waves propagating in the indefinite medium with the tilted optical axis. This condition does not depend on the frequency while $\varepsilon_t = 1$, which is satisfied for arrays of thin single-wall metallic CNTs. Then, taking into account that $|k_z^{(2)}| \to \infty$, we come to condition of perfect absorption if the indefinite medium possesses low losses. In this case the wave, propagating in the slab with a very short wavelength, attenuates at an ultrashort distance. The frequency dependence of the real part of the wave impedance of the CNT array is shown in Fig. 7. Despite that all nonzero components of the permittivity dyadic quite strongly depend on the frequency, the real part of $Z_{1,2}$ remains constant within the whole frequency range jumping from -1 to 1 (or vice versa) at $f = f_p$. The imaginary part of $Z_{1,2}$ is close to zero under the parameter of losses taken here.

III. PLANE-WAVE REFLECTION FROM A GROUNDED SLAB OF TILTED CARBON NANOTUBES

For solution of the wave reflection problem we will use the 2×2 transfer matrix method, modified for the general case $|k_z^1| \neq |k_z^2|$. Propagation constants and transverse wave impedances of the waves within the slab can be expressed via elements of the transfer matrix $[M]$ as[25]

$$e^{-jk_z^{(1,2)}h} = \frac{M_{11} + M_{22} \pm \sqrt{(M_{11} + M_{22})^2 - 4|M|}}{2},$$
$$Z_{1,2} = \frac{M_{12}}{M_{11} - e^{-jk_z^{1,2}h}}, \tag{18}$$

where $|M|$ is the determinant of the transfer matrix. Solving the system of equations with respect to M_{ij} one can obtain the expression for the transfer matrix via the wave impedances and wave numbers as

$$\overline{\overline{M}} = \begin{bmatrix} M_{11} & M_{12} \\ M_{21} & M_{22} \end{bmatrix} = \begin{bmatrix} \frac{Z_1 e^{-jk_z^{(1)}h} - Z_2 e^{-jk_z^{(2)}h}}{Z_1 - Z_2} & -Z_1 Z_2 \frac{e^{-jk_z^{(1)}h} - e^{-jk_z^{(2)}h}}{Z_1 - Z_2} \\ \frac{e^{-jk_z^{(1)}h} - e^{-jk_z^{(2)}h}}{Z_1 - Z_2} & \frac{Z_2 e^{-jk_z^{(1)}h} - Z_1 e^{-jk_z^{(2)}h}}{Z_2 - Z_1} \end{bmatrix}. \tag{19}$$

The reflection coefficient R can be calculated using the well-known formula

$$R = \frac{M_{12} - M_{22} Z_0}{M_{12} + M_{22} Z_0}, \tag{20}$$

where Z_0 is defined by formula (17). Absorption A is defined as

$$A = 1 - |R|^2. \tag{21}$$

The frequency dependence of absorption A is shown in Fig. 8. It is remarkable that the thickness resonance is absent due to the difference in propagation constants for upward and downward waves within the slab. The central frequency of the absorption band $f_0 = 20$ THz corresponds to the IM condition which is determined by the period of the CNT array lattice. Increase of the thickness causes increase of the absorption bandwidth. The total absorption bandwidth of 17% can be achieved at the thickness 3.75 μm ($0.25\lambda_0$) and 8.6% at $h = 0.1\lambda_0$. The incidence angle dependence of the absorption, calculated for different frequencies in vicinity of f_0, is shown in Fig. 9. At the IM frequency f_0 the total absorption is achieved at $\theta = \pm 45^\circ$. However, if the operating frequency is slightly different from f_0, the level of absorption around 95% can be achieved within the range $-60^\circ < \theta < 60^\circ$.

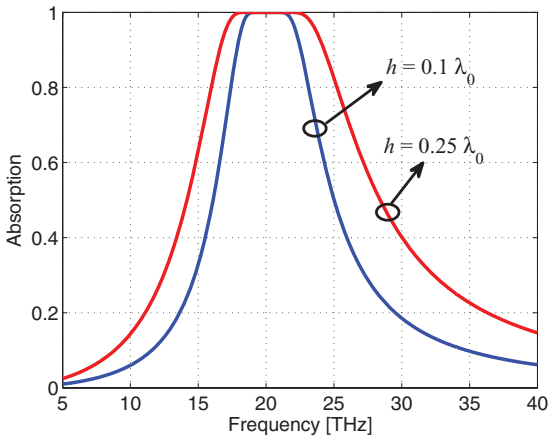

FIG. 8. (Color online) Absorption versus frequency calculated for different thicknesses of the slab. The incidence angle is 45°, the tilt angle is 45°, and λ_0 is the wavelength in free space corresponding to f_0.

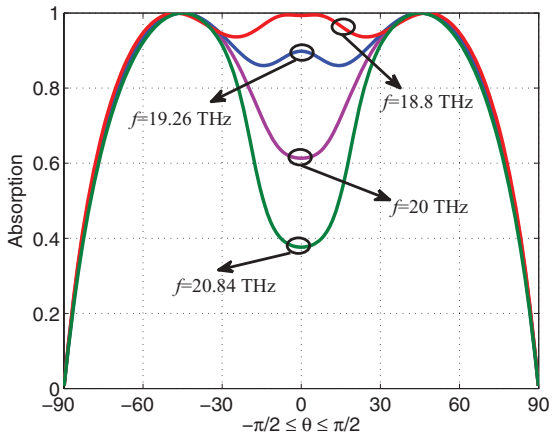

FIG. 9. (Color online) Absorption versus the incidence angle.

IV. CONCLUSION

We proposed an alternative, based on a plasmonic resonance solution, for design of optically thin absorbing layers. It exploits properties of a specially prepared indefinite medium, whose permittivity tensor has near-zero diagonal components and close to −1 nondiagonal components. The wave, incident under the angle 45°, enters the slab without reflection and propagates, attenuating in the medium with a very small wavelength that provides perfect absorption within ultrathin layers. We have demonstrated that such absorbing slabs for the mid-infrared range can be made of arrays of metallic carbon nanotubes, which possess properties of indefinite media in the terahertz range.[13] The discussed effect can find applications for such absorbers, where a range of incidence angles is confined.

ACKNOWLEDGMENTS

The first author would like to thank Iran's MSRT (The Ministry of Science, Research and Technology) and ITRC (Iran Telecommunications Research Center) for their financial support during the visit to Aalto University (Finland). This work has been partially funded by the Academy of Finland and Nokia through the Center-of-Excellence program.

[1]D. Yu. Shchegolkov, A. K. Azad, J. F. O'Hara, and E. I. Simakov, Phys. Rev. B **82**, 205117 (2010).
[2]M. Diem, T. Koschny, and C. M. Soukoulis, Phys. Rev. B **79**, 033101 (2009).
[3]K. B. Alici, A. B. Turhan, C. M. Soukoulis, and E. Ozbay, Opt. Express **19**, 14260 (2011).
[4]C. H. Lin, R. L. Chern, and H. Y. Lin, Opt. Express **19**, 415 (2011).
[5]N. I. Landy, S. Sajuyigbe, J. J. Mock, D. R. Smith, and W. J. Padilla, Phys. Rev. Lett. **100**, 207402 (2008).
[6]H. Tao, N. I. Landy, C. M. Bingham, X. Zhang, R. D. Averitt, and W. J. Padilla, Opt. Express **16**, 7181 (2008).
[7]H.-T. Chen, Opt. Express **20**, 7165 (2012).
[8]S. Kivistö, T. Hakulinen, A. Kaskela, B. Aitchison, D. P. Brown, A. G. Nasibulin, E. I. Kauppinen, A. Härkönen, and O. G. Okhotnikov, Opt. Express **17**, 2358 (2009).
[9]Jin-Chen Chiu *et al.*, Opt. Express **18**, 3592 (2010).
[10]J. H. Lehman, B. Lee, and E. N. Grossman, Appl. Optics **50**, 4099 (2011).
[11]K. Mizuno, J. Ishii, H. Kishida, Y. Hayamizu, S. Yasuda, D. N. Futaba, M. Yamura, and K. Hata, Proc. Natl. Acad. Sci. USA **106**, 6044 (2009)
[12]I. S. Nefedov, Phys. Rev. B **82**, 155423 (2010).
[13]I. S. Nefedov and S. A. Tretyakov, Phys. Rev. B **84**, 113410 (2011).
[14]D. R. Smith and D. Schurig, Phys. Rev. Lett. **90**, 077405 (2003).
[15]G. Y. Slepyan, S. A. Maksimenko, A. Lakhtakia, O. Yevtushenko, and A. V. Gusakov, Phys. Rev. B **60**, 17136 (1999).
[16]I. S. Nefedov and S. A. Tretyakov, Photonics Nanostruct. **9**, 374 (2011).
[17]P. J. Burke, S. Li, and Z. Yu, IEEE Trans. Nanotechnol. **5**, 314 (2006).
[18]G. W. Hanson, IEEE Trans. Microwave Theory Tech. **59**, 9 (2011).
[19]J. Hao and G. W. Hanson, Phys. Rev. B **74**, 035119 (2006).
[20]A. Maffucci, G. Miano, and F. Villone, Int. J. Circ. Theor. Appl. **36**, 31 (2008).
[21]G. Miano and F. Villone, IEEE Trans. Antennas Propag. **54**, 2713 (2006).
[22]S. M. Mikki and A. A. Kishk, IEEE Trans. Antennas Propag. **57**, 1412 (2009).
[23]G. Miano, C. Forestiere, A. Maffucci, S. A. Maksimenko, G. Ya. Slepyan, IEEE Trans. Nanotechnol. **10**, 135 (2011).
[24]S. I. Maslovski and M. G. Silveirinha, Phys. Rev. B **80**, 245101 (2009).
[25]D. M. Pozar, *Microwave Engineering*, 3rd ed. (Wiley, New York, 2009).